Matsubara *et al. Journal of Wood Science* (2022) 68:53
https://doi.org/10.1186/s10086-022-02060-3

Journal of Wood Science

NOTE

Open Access

Elastic interaction in multiple bolted timber joints

Doppo Matsubara[1*], Masaki Teranishi[2] and Yoshiaki Wakashima[3]

Abstract

The management of axial forces is an important issue when a joining method that takes into account the axial forces generated by tightening bolts is applied to the bolted joints of a wooden structure during construction. This study focuses on elastic interactions in which the axial force of adjacent bolts changes as a result of sequential tightening of each bolt in multiple bolted joints affecting the deformation around each of the other bolts. To this end, tightening experiments are conducted within the elastic range, with the tightening sequence, bolt spacing, and wood thickness set as parameters. From the results, it was found that variations in axial force tended to decrease as bolt spacing increases. In addition, an evaluation formula for calculating fluctuations in axial force due to elastic interactions was derived. By comparing the calculated value to the experimental value, it was found that as bolt spacing was increased, the calculated value tended to capture the experimental values well.

Keywords: Elastic interaction, Bolted timber joints, Tightening sequence, Embedment stiffness, Metal washer

Introduction

Bolted joints are the most typical kind of joint in wooden structures [1]. During construction, when bolts are tightened using a tool, such as a torque wrench, an axial force is generated in the axial direction of the bolt. This axial force cannot be maintained for a long period because of stress relaxation and drying shrinkage of wood and is currently not taken into account during joint design [2, 3]. However, recent research has reported that, when bolts are tightened to reach the plastic region of wood and are tightened in the direction of the grain of wood and wood-based materials, a high axial force is maintained over a long period of time, even if subjected to the effects of repeated drying and wetting [4, 5]. Research and development regarding wood friction connectors and prestressed timber joints that utilize this axial force is currently underway and the authors have reported on the high seismic performance of bearing walls incorporating wood friction connectors and the joint performance of prestressed timber joints [6–9].

However, to implement these joining methods in actual buildings, it is important to maintain the axial force for a long period of time, and, in addition, axial force management during construction is also an important issue. Thus far, the authors have revealed, with regard to axial force management, that the so-called torque method, which manages wood joints using a single bolt or a single lag screw with a tool, such as a torque wrench, can be applied and that axial force generated while tightening a lag screw is lower than the pull-out strength of the lag screw, owing to the effects of friction at the threaded part [10–14]. However, for joint types formed with multiple bolts, such as the wood friction connectors proposed by the authors, sequential tightening of each bolt affects deformation around each of the other bolts. This leads to elastic interactions in which the axial force of adjacent bolts changes. This is considered to be a problem, because the axial force of bolts in bolted joints formed from a metallic material cannot be uniform, since variations in axial force due to these elastic interactions are unavoidable. Analytical and experimental studies on

*Correspondence: d.matsubara@fuk.kindai.ac.jp

[1] Kindai University, 11-6 Kayanomori, Iizuka, Fukuoka 820-8555, Japan
Full list of author information is available at the end of the article

tightening sequences have tried to minimize variations in the mechanism of the elastic interactions and in the axial force [15–25]. However, research into elastic interactions in bolted joints of wooden structures has not been found, so it is necessary to proceed with basic research on the implementation of the above-mentioned wood friction connectors in actual buildings.

In the present study, as a first step toward such basic research into elastic interactions in bolted joints of wooden structures, tightening experiments within an elastic range were performed to ascertain the effects of the tightening sequence, bolt spacing, and wood thickness on fluctuations in axial force. Furthermore, an evaluation formula for calculating fluctuations in axial force due to elastic interactions was derived using the embedment stiffness of the washers [26–28], and the extent to which the calculated value captures the experimental value was also considered.

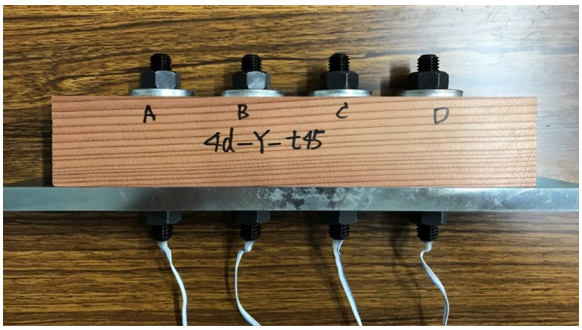

Fig. 2 Typical test piece (*S*: 48 mm; T_h: 45 mm)

Materials and methods

Tightening test

Figure 1 shows the outline of the experiments and Fig. 2 shows the state of a typical test piece. Japanese Cedar (*Cryptomeria japonica*) was selected as the wood. M12, S45C steel bolts with a pitch of 1.75 mm and double-ended thread were selected. Round, SPCC steel washers with a diameter of 35 mm, thickness of 4.5 mm, and bolt hole diameter of 13.5 mm were selected. S45C steel nuts for M12 bolts were selected. Four levels of bolt spacing *S*, namely, 48, 60, 72, and 84 mm were selected (these dimensions correspond to 4d, 5d, 6d, and 7d (where d is the bolt diameter). Three levels of wood thickness T_h were selected, namely, 30, 45, and 60 mm, and one test piece was used for each experiment (for a total of twelve). The density and moisture content of the test pieces are shown in Table 1. Four tightening sequences were selected, as shown in Fig. 1, namely, Se.1: A → B → C → D; Se.2: A → D → B → C; Se.3: A → C → B → D; and Se.4: B → C → A → D. Axial force was measured with a strain gauge inserted into a ϕ2 mm hole made in the center of the bolt. Note that this bolt was subjected to the tightening experiment after calibrating the axial force with a universal testing machine. The initial axial force of the bolt was set to 2 kN, which is estimated to be within the elastic range [11], and tightened with a torque wrench. Once the axial force reached 2 kN, tightening was stopped and,

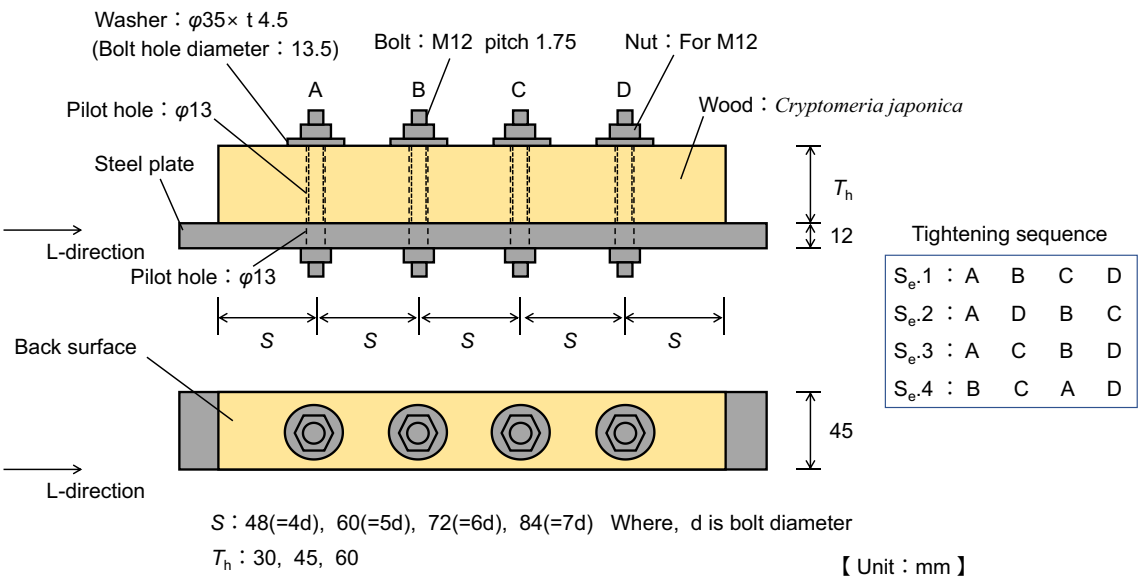

Fig. 1 Schematic of the apparatus for the tightening test (L: longitudinal)

Table 1 Basic properties of tightening test materials

T_h [mm]	S [mm]	Density [kg / m^3]	Moisture content [%]
30	48	390	10.3
	60	347	10.1
	72	353	10.5
	84	402	10.4
45	48	371	11.1
	60	367	10.8
	72	369	10.4
	84	392	10.5
60	48	368	10.3
	60	372	10.2
	72	380	10.7
	84	370	10.0

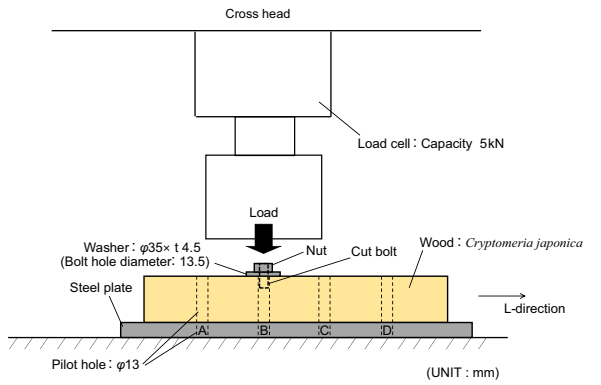

Fig. 3 Schematic of the apparatus for the embedment test of metal washers (L: longitudinal)

after waiting for 1 min, the next bolt was tightened. The tightening direction was set perpendicular to the grain.

Embedment test of metal washers

To obtain the embedment stiffness K_{ew} of the washers, embedment tests were performed on the washers at each bolt location (A, B, C, and D) in the test piece used in the tightening experiment. In the experiment, a universal testing machine (AG-50kNX-Plus, Shimadzu Corporation, Japan) was used to monotonically load up to 2 kN perpendicular to the grain, as shown in Fig. 3. The test speed was 1 mm/min. The amount of displacement was determined by the amount of movement of the crosshead. From the relationship between load and displacement that was obtained, the secant gradients of 1.0 kN and 2.0 kN were calculated and used as K_{ew}.

Results and discussion

Residual axial bolt force

Figure 4 shows typical results for the axial bolt force ratio over time for a test piece with a thickness T_h of 30 mm and a bolt spacing S of 48 mm. Here, the axial force ratio is calculated using

$$\alpha = \frac{F_T}{F_f} \tag{1}$$

where F_f is the initial axial force (2 kN) and F_T is the axial force T [s] thereafter.

First, looking at Se.1, it can be seen that when the bolts are tightened in this order, the axial force of the previously tightened bolts is reduced by approximately 16% upon completion of tightening. This trend is also observed in Se.2. After all the bolts have been tightened in Se. 1 and Se.2, the bolt tightened last (i.e., bolt D and C in Se. 1 and Se. 2, respectively) has different axial force ratio of other bolts. However, looking at C in Se.3 and B in Se.4 reveals that tightening the two bolts adjacent to bolts results in the axial force ratio decreasing twice, and unlike in Se.1 and Se.2, where the axial force ratio was not uniform after all the bolts had been tightened, the variation in axial force ratio was large. Furthermore, a difference can be observed between the first and the second decreases in the axial force ratio of bolt B in Se.4.

Tables 2, 3, and 4 show the axial force ratios of all bolts after tightening. The tables also include the ratio between the maximum and minimum axial force ratio as *Max./Min.* First, with regard to $T_h = 30$ mm in Table 2, there is a tendency for *Max./Min.* to decrease as the bolt spacing S is increased. This indicates that the axial forces of all the bolts are approximately uniform. Next, as shown in Table 3, *Max./Min.* for $T_h = 45$ mm becomes higher than that for $T_h = 30$ mm, and for $S = 48$ mm, the *Max./Min.* value in Se.3 and Se.4 is four times higher than for $T_h = 30$ mm. In particular, both of bolt C of Se. 3 and bolt B of Se. 4 are affected by two decreases in axial force, resulting in respective axial forces of 0.17 and 0.16, which can be understood to cause the large *Max./Min.* However, the *Max./Min.* for $S = 84$ mm ranged from 1 to 1.1, regardless of the tightening sequence, which was the same as for $T_h = 30$ mm. However, it is difficult to conclude that there is an explicit relationship between bolt spacing and *Max./Min.* Similarly, as shown in Table 4, *Max./Min.* for $T_h = 60$ mm becomes higher than that for $T_h = 30$ mm in a similar manner as for $T_h = 45$ mm. For $S = 84$ mm, the *Max./Min.* range is 1.26 to 1.68, which is a large variation compared to the ranges for $S = 84$ mm for $T_h = 30$ mm or $T_h = 45$ mm.

Figure 5 shows the relationship between *Max./Min.* and S for each tightening sequences. According to Fig. 5, *Max./Min.* tended to decrease as S increased regardless

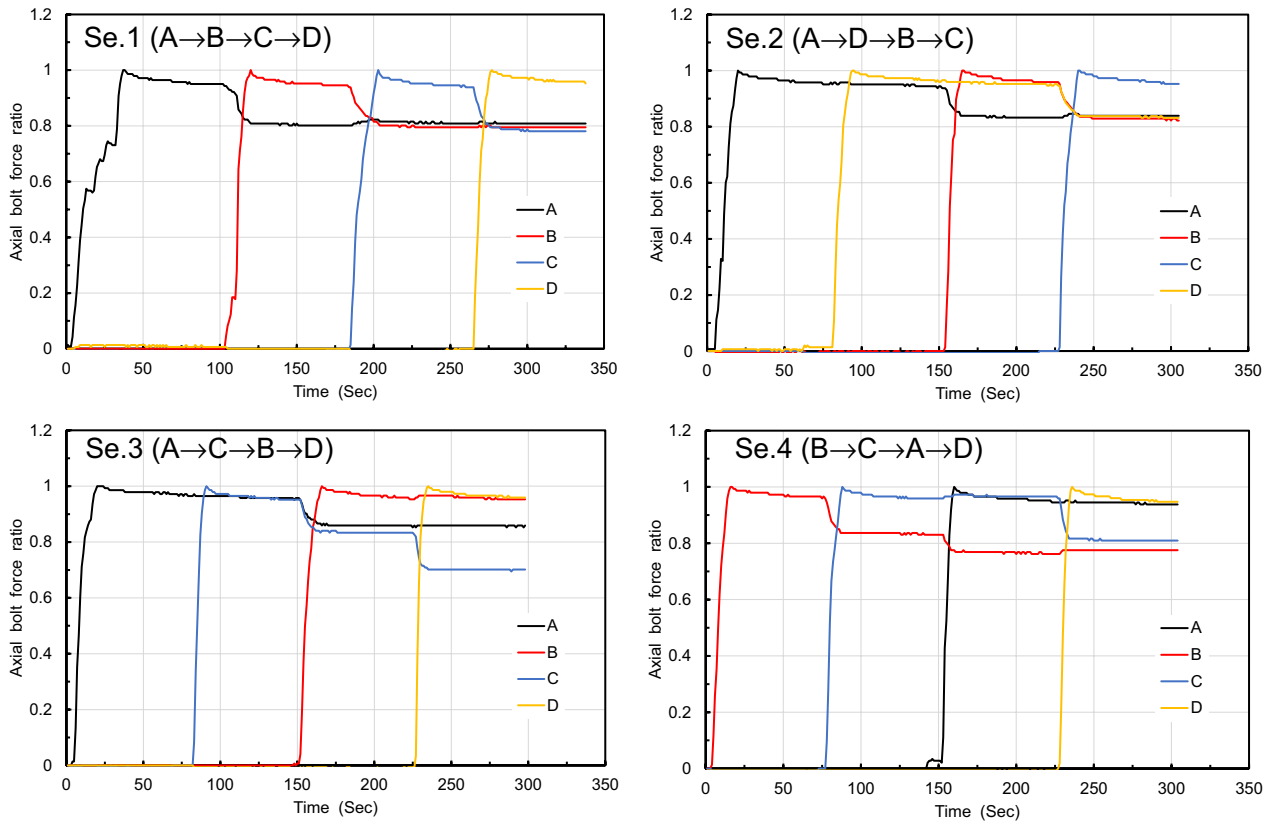

Fig. 4 Relationship between axial bolt force ratio and time (T_h: 30 mm, S: 48 mm)

of T_h and tightening sequences. On the other hand, no clear trend was observed between *Max./Min.* and T_h. These results suggest that, within the scope of these experiments, when S is increased, a suppression in variation of axial forces due to elastic interactions can be expected, regardless of which tightening sequence is employed.

Calculation of axial bolt force ratio under elastic interaction

As mentioned above, bolt spacing greatly affect variations in axial force due to elastic interactions and it is assumed that the embedment stiffness of a metal washer is closely related to it. Washer embedment stiffness greatly depends on the side length ratio of the washer (washer's side length to thickness) [27, 28]. The side length ratios of the washers used in these experiments were 7.8 (35 mm/4.5 mm $\approx$ 7.8) and for such side length ratios, it is considered that there is almost no bending deformation of the washers due to bolt tightening [11, 27, 28]. It is also assumed that the washer became embedded into the wood side while maintaining an almost rectangular shape (a state in which the washer can be regarded as a rigid body). Figure 6 shows a diagram of the deformation when bolts are tightened with washers, which are assumed to be rigid bodies. As mentioned above experimental results, when evaluating the bolt axial force ratio, it is sufficient to consider the influence of two adjacent bolts, and three bolts are joined. First, as shown in Fig. 6a, when bolt 1 is tightened by an initial axial force F_1, a deformation δ_1 occurs directly beneath the washer. Next, as shown in (b), when bolt 2 is tightened by a force F_1, the deformation directly beneath the washer of bolt 1 is affected by the deformation directly beneath the washer of bolt 2, thus changing the deformation δ_1 to $\delta_{1,2}$ and changing the axial force to $F_{1,2}$. Furthermore, as shown in (c), when bolt 3 is tightened by a force F_1, the deformation directly beneath the washer of bolt 1 is affected by the deformation directly beneath the washer of bolt 3, thus changing the deformation $\delta_{1,2}$ to $\delta_{2,3}$ and changing the axial force to $F_{2,3}$. An evaluation formula for the axial force ratio α is derived from this deformation diagram. Note that changes in axial force due to stress relaxation and creep of wood were not taken into account when deriving the evaluation formula in this study. First, the deformed shape of the additional length part in the direction of the grain from the washer end is expressed as an exponential curve, and if it is further assumed that the length from the end of the washer to a position, where becomes almost zero is 1.5 times the

Table 2 List of axial bolt force ratios after tightening all bolts (T_h: 30 mm)

T_h [mm]	S [mm]	Bolt Number	Axial bolt force ratio			
			Se.1 A → B → C → D	Se.2 A → D → B → C	Se.3 A → C → B → D	Se.4 B → C → A → D
30	48	A	0.81	0.84	0.86	0.94
		B	0.79	0.82	0.95	0.78
		C	0.78	0.95	0.70	0.81
		D	0.95	0.83	0.96	0.95
		Max./Min	1.22	1.16	1.37	1.22
	60	A	0.76	0.78	0.79	0.91
		B	0.75	0.82	0.90	0.74
		C	0.84	0.90	0.78	0.84
		D	0.91	0.87	0.93	0.93
		Max./Min	1.22	1.15	1.19	1.25
	72	A	0.80	0.83	0.85	0.90
		B	0.78	0.86	0.91	0.78
		C	0.75	0.88	0.74	0.83
		D	0.88	0.83	0.91	0.92
		Max./Min	1.18	1.07	1.23	1.18
	84	A	0.89	0.90	0.89	0.91
		B	0.88	0.92	0.91	0.92
		C	0.88	0.92	0.90	0.90
		D	0.88	0.86	0.90	0.93
		Max./Min	1.02	1.06	1.03	1.03

Table 3 List of axial bolt force ratios after tightening all bolts (T_h: 45 mm)

T_h [mm]	S [mm]	Bolt Number	Axial bolt force			
			Se.1 A → B → C → D	Se.2 A → D → B → C	Se.3 A → C → B → D	Se.4 B → C → A → D
45	48	A	0.64	0.57	0.55	0.96
		B	0.55	0.54	0.92	0.16
		C	0.44	0.92	0.17	0.57
		D	0.93	0.57	0.94	0.93
		Max./Min	2.12	1.70	5.61	6.01
	60	A	0.85	0.89	0.89	0.94
		B	0.82	0.86	0.92	0.81
		C	0.84	0.91	0.81	0.89
		D	0.89	0.85	0.93	0.94
		Max./Min	1.08	1.07	1.15	1.16
	72	A	0.77	0.81	0.77	0.93
		B	0.73	0.73	0.94	0.65
		C	0.73	0.94	0.61	0.78
		D	0.91	0.77	0.91	0.93
		Max./Min	1.26	1.29	1.55	1.42
	84	A	0.85	0.90	0.89	0.92
		B	0.88	0.91	0.93	0.92
		C	0.92	0.95	0.95	0.94
		D	0.93	0.92	0.94	0.94
		Max./Min	1.09	1.05	1.07	1.02

Table 4 List of axial bolt force ratios after tightening all bolts (T_h: 60 mm)

T_h [mm]	S [mm]	Bolt Number	Axial bolt force			
			Se.1 A → B → C → D	Se.2 A → D → B → C	Se.3 A → C → B → D	Se.4 B → C → A → D
60	48	A	0.68	0.62	0.54	0.98
		B	0.49	0.50	0.93	0.17
		C	0.48	0.94	0.21	0.56
		D	0.94	0.49	0.94	0.93
		Max./Min	1.95	1.90	4.57	5.81
	60	A	0.71	0.68	0.61	0.97
		B	0.58	0.59	0.98	0.33
		C	0.57	0.94	0.29	0.64
		D	0.95	0.57	0.96	0.95
		Max./Min	1.65	1.66	3.42	2.95
	72	A	0.84	0.87	0.86	0.93
		B	0.81	0.83	0.94	0.77
		C	0.75	0.92	0.72	0.84
		D	0.92	0.83	0.94	0.94
		Max./Min	1.22	1.11	1.31	1.23
	84	A	0.78	0.81	0.78	0.95
		B	0.76	0.77	0.96	0.62
		C	0.72	0.95	0.57	0.78
		D	0.92	0.75	0.95	0.95
		Max./Min	1.28	1.26	1.68	1.52

wood thickness T_h, then the function can be expressed as [29]

$$f(x) = \delta_i e^{-\frac{3}{2T_h}x} \tag{2}$$

where x is the distance from the washer end and δ_i is the amount of deformation directly beneath the washer. This can be calculated using the embedment stiffness K_{ewi} of the washer and initial axial force F_i:

$$\delta_i = \frac{F_i}{K_{ewi}} \tag{3}$$

Here, $\delta_{1,2}$ of Fig. 6 can be calculated from Eq. (4) using the amount of change in axial force $\Delta F_{1,2}$ [22] of bolt 1 due to tightening of bolt 2 and Eqs. (2) and (3):

$$\delta_{1,2} = \frac{\Delta F_{1,2}}{K_{ew1}} + \frac{F_1}{K_{ew2}} e^{-\frac{3}{2T_h}(S-\varphi)} \tag{4}$$

Similarly, $\delta_{2,3}$ can be calculated using the amount of change in axial force $\Delta F_{2,3}$ [22] of bolt 1 due to tightening of bolt 3 after tightening bolt 2:

$$\delta_{2,3} = \frac{\Delta F_{2,3}}{K_{ew1}} + \frac{F_1}{K_{ew2}} e^{-\frac{3}{2T_h}(S-\varphi)} + \frac{F_1}{K_{ew3}} e^{-\frac{3}{2T_h}(S-\varphi)} \tag{5}$$

From the compatibility conditions of the elastic deformation, Eqs. (6) and (7) hold using the bolt elongation δ_{b1}:

$$\delta_{1,2} + \delta_{b1} = \frac{\Delta F_{1,2}}{K_{ew1}} + \frac{F_1}{K_{ew2}} e^{-\frac{3}{2T_h}(S-\varphi)} + \frac{\Delta F_{1,2}}{K_{b1}} = 0 \tag{6}$$

$$\delta_{2,3} + \delta_{b1} = \frac{\Delta F_{2,3}}{K_{ew1}} + \frac{F_1}{K_{ew2}} e^{-\frac{3}{2T_h}(S-\varphi)} + \frac{F_1}{K_{ew3}} e^{-\frac{3}{2T_h}(S-\varphi)} + \frac{\Delta F_{2,3}}{K_{b1}} = 0 \tag{7}$$

Here, K_{b1} is the stiffness of the bolt and can be calculated by the equation in Ref. [30]. The sums $\delta_{1,2}+\delta_{b1}$ and $\delta_{2,3}+\delta_{b1}$ can be calculated from Eqs. (6) and (7), respectively, and $\Delta F_{1,2}$ and $\Delta F_{2,3}$ can be calculated from Eqs. (8) and (9), respectively:

$$\Delta F_{1,2} = -F_1 e^{-\frac{3}{2T_h}(S-\varphi)} \frac{1}{\left(\frac{1}{K_{ew1}} + \frac{1}{K_{b1}}\right) K_{ew2}} \tag{8}$$

$$\Delta F_{2,3} = -F_1 e^{-\frac{3}{2T_h}(S-\varphi)} \frac{\left(\frac{1}{K_{ew2}} + \frac{1}{K_{ew3}}\right)}{\left(\frac{1}{K_{ew1}} + \frac{1}{K_{b1}}\right)} \tag{9}$$

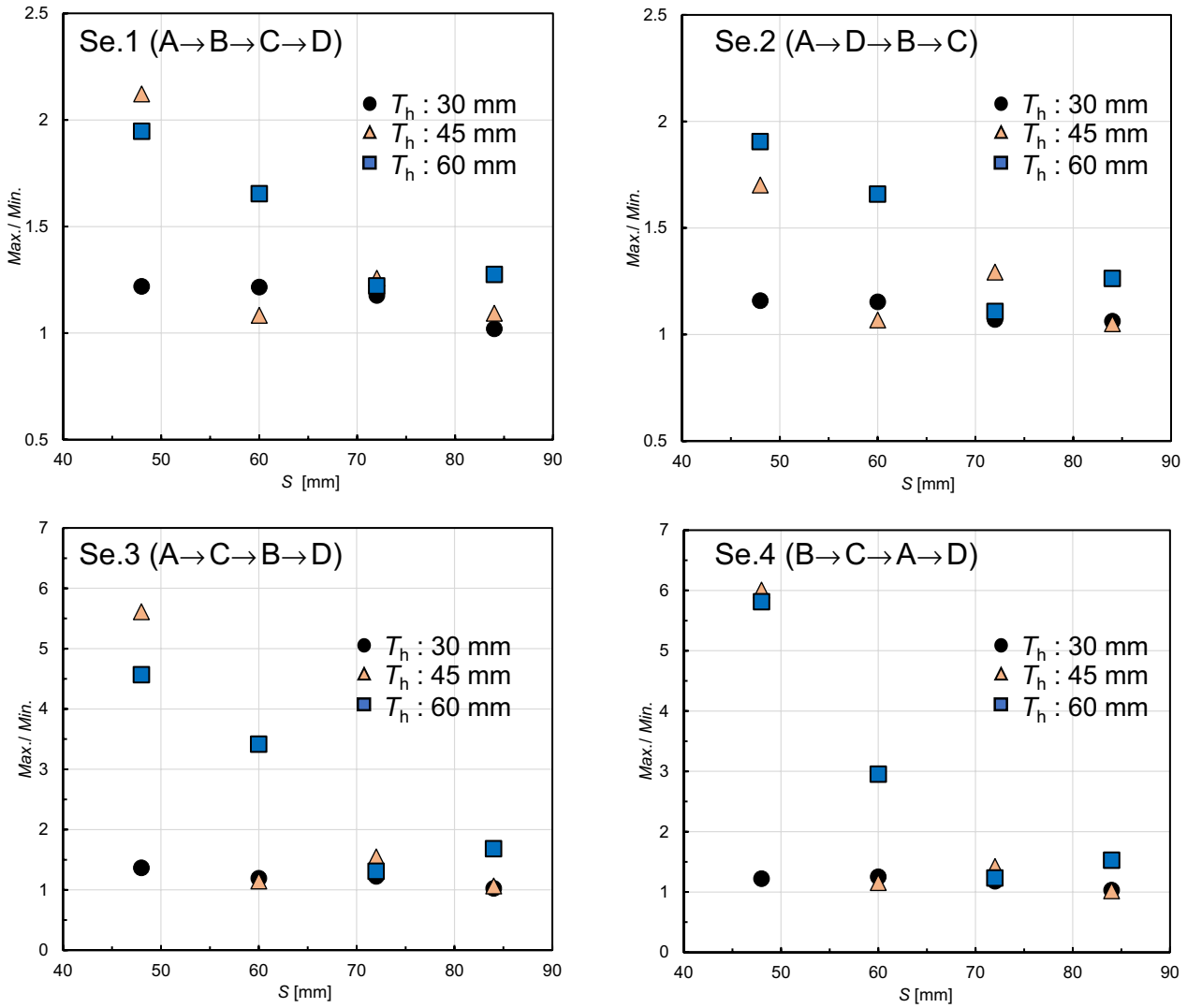

Fig. 5 Relationship between *Max./Min.* and *S*

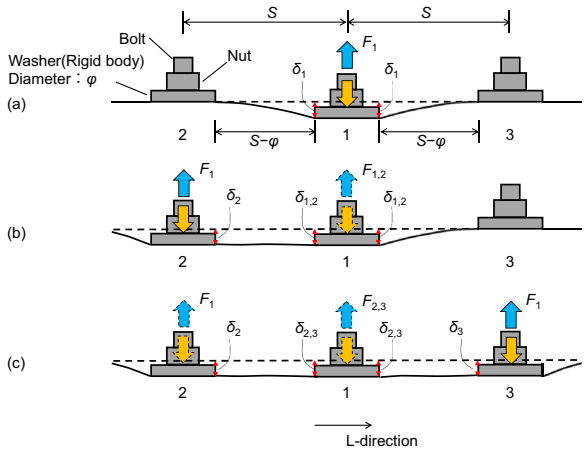

Fig. 6 Diagram of deformation when tightening bolts. (**a**) When bolt 1 is tightened, (**b**) When bolt 2 is tightened, (**c**) When bolt 3 is tightened

Therefore, the axial force ratio α of bolt 1 in Fig. 6b, c can be calculated from Eqs. (10) and (11), respectively.

The axial force ratio α of bolt 1 in Fig. 6b is

$$\alpha = \frac{(F_1 + \Delta F_{1,2})}{F_1} \tag{10}$$

and the axial force ratio α of bolt 1 in Fig. 6c is

$$\alpha = \frac{(F_1 + \Delta F_{2,3})}{F_1} \tag{11}$$

The axial force ratio α was calculated from the above series of equations and compared with the experimental results. Table 5 shows a list of values for the washer embedment stiffness K_{ew} obtained from the washer embedment experiment for use in the calculations. Tables 6,7 and 8 show a comparison between

Table 5 Results for embedment stiffness of a metal washer into a timber member

Bolt Number	T_h [mm]											
	30				45				60			
	S [mm]											
	48	60	72	82	48	60	72	82	48	60	72	82
	K_{ew} [kN/mm]											
A	10.0	8.4	6.8	11.9	4.7	12.4	7.2	9.0	5.2	5.8	11.4	5.8
B	12.3	8.2	6.4	11.3	5.4	13.0	5.1	11.3	6.0	6.1	10.4	5.6
C	13.3	8.9	6.5	10.4	5.4	10.0	4.9	12.8	6.0	5.7	9.8	5.7
D	13.9	10.6	6.4	10.2	4.9	12.8	4.9	14.4	5.4	5.7	10.8	5.9

calculation values and experimental values. Note that Se.3 (bolt C) and Se.4 (bolt B) for $T_h = 30$ and 45 mm and $S = 48$ mm, and Se.3 (bolt C) and Se. 4 (bolt B) for $T_h = 60$ mm and $S = 48$ and 60 mm produced a negative value, and Cal./Exp. is recorded as "0.00". Furthermore, after tightening, a decrease in axial force of several percent due to stress relaxation and creep over time is confirmed, as shown in Fig. 4. However, it is considered that this decrease in axial force due to stress relaxation and creep is also included in the fluctuations in axial force due to elastic interactions. As such, when comparing the experimental values with the calculated values from the proposed evaluation formula, which does not consider stress relaxation and creep into account, it is appropriate for the experimental value to also exclude this stress relaxation and creep. However, it is assumed that the stress relaxation and creep characteristics differ depending on the variation of the wood material directly beneath each washer or on the tightening speed [31] and conducting an evaluation excluding stress relaxation and creep is very difficult. As such, in this study, the experimental values were set to include stress relaxation and creep and were set to

Table 6 Comparison between experimental results and calculation results for axial bolt force ratio (T_h: 30 mm)

T_h [mm]	*S* [mm]	Bolt Number	Axial bolt force ratio											
			Se.1 A → B → C → D			Se.2 A → D → B → C			Se.3 A → C → B → D			Se.4 B → C → A → D		
			Exp.	*Cal.*	*Cal./Exp.*	*Exp.*	*Cal.*	*Cal./Exp.*	*Exp.*	*Cal.*	*Cal./Exp.*	*Exp.*	*Cal.*	*Cal./Exp.*
30	48	A	0.81	0.59	0.73	0.84	0.59	0.70	0.86	0.59	0.68	–	–	–
		B	0.79	0.54	0.68	0.82	0.54	0.65	–	–	–	0.78	− 0.08	0.00
		C	0.78	0.52	0.67	–	–	–	0.70	− 0.02	0.00	0.81	0.52	0.64
		D	–	–	–	0.83	0.48	0.58	–	–	–	–	–	–
	60	A	0.76	0.72	0.94	0.78	0.72	0.91	0.79	0.72	0.91	–	–	–
		B	0.75	0.74	0.99	0.82	0.74	0.90	–	–	–	0.74	0.47	0.63
		C	0.84	0.77	0.91	–	–	–	0.78	0.47	0.60	0.84	0.77	0.91
		D	–	–	–	0.87	0.67	0.77	–	–	–	–	–	–
	72	A	0.80	0.84	1.05	0.83	0.84	1.01	0.85	0.84	0.98	–	–	–
		B	0.78	0.84	1.07	0.86	0.85	0.99	–	–	–	0.78	0.71	0.90
		C	0.75	0.85	1.13	–	–	–	0.74	0.68	0.92	0.83	0.84	1.01
		D	–	–	–	0.83	0.85	1.03	–	–	–	–	–	–
	84	A	0.89	0.91	1.02	0.90	0.91	1.02	0.89	0.91	1.02	–	–	–
		B	0.88	0.91	1.04	0.92	0.91	0.99	–	–	–	0.92	0.83	0.91
		C	0.88	0.91	1.04	–	–	–	0.90	0.84	0.94	0.90	0.91	1.02
		D	–	–	–	0.86	0.92	1.06	–	–	–	–	–	–

Table 7 Comparison between experimental results and calculation results for axial bolt force ratio (T_h: 45 mm)

T_h [mm]	S [mm]	Bolt Number	Axial bolt force ratio											
			Se.1 A → B → C → D			Se.2 A → D → B → C			Se.3 A → C → B → D			Se.4 B → C → A → D		
			Exp.	*Cal.*	*Cal./Exp.*	*Exp.*	*Cal.*	*Cal./Exp.*	*Exp.*	*Cal.*	*Cal./Exp.*	*Exp.*	*Cal.*	*Cal./Exp.*
45	48	A	0.64	0.45	0.70	0.57	0.45	0.78	0.55	0.45	0.81	–	–	–
		B	0.55	0.37	0.68	0.54	0.37	0.68	–	–	–	0.16	− 0.36	0.00
		C	0.44	0.29	0.67	–	–	–	0.17	− 0.34	0.00	0.57	0.29	0.52
		D	–	–	–	0.57	0.43	0.75	–	–	–	–	–	–
	60	A	0.85	0.61	0.71	0.89	0.61	0.68	0.89	0.61	0.68	–	–	–
		B	0.82	0.46	0.56	0.86	0.46	0.54	–	–	–	0.81	0.03	0.04
		C	0.84	0.68	0.80	–	–	–	0.81	0.36	0.44	0.89	0.52	0.58
		D	–	–	–	0.85	0.47	0.55	–	–	–	–	–	–
	72	A	0.77	0.60	0.78	0.81	0.60	0.75	0.77	0.60	0.78	–	–	–
		B	0.73	0.70	0.96	0.73	0.70	0.96	–	–	–	0.65	0.50	0.76
		C	0.73	0.72	0.99	–	–	–	0.61	0.44	0.73	0.78	0.72	0.92
		D	–	–	–	0.77	0.71	0.93	–	–	–	–	–	–
	84	A	0.85	0.85	0.99	0.90	0.85	0.94	0.89	0.85	0.95	–	–	–
		B	0.88	0.83	0.95	0.91	0.83	0.92	–	–	–	0.92	0.60	0.65
		C	0.92	0.84	0.91	–	–	–	0.95	0.63	0.66	0.94	0.84	0.89
		D	–	–	–	0.92	0.79	0.86	–	–	–	–	–	–

Table 8 Comparison between experimental results and calculation results for axial bolt force ratio (T_h: 60 mm)

T_h [mm]	S [mm]	Bolt Number	Axial bolt force ratio											
			Se.1 A → B → C → D			Se.2 A → D → B → C			Se.3 A → C → B → D			Se.4 B → C → A → D		
			Exp.	*Cal.*	*Cal./Exp.*	*Exp.*	*Cal.*	*Cal./Exp.*	*Exp.*	*Cal.*	*Cal./Exp.*	*Exp.*	*Cal.*	*Cal./Exp.*
60	48	A	0.68	0.39	0.57	0.62	0.39	0.63	0.54	0.39	0.72	–	–	–
		B	0.49	0.30	0.61	0.50	0.30	0.60	–	–	–	0.17	− 0.51	0.00
		C	0.48	0.21	0.44	–	–	–	0.21	−0.49	0.00	0.56	0.21	0.38
		D	–	–	–	0.49	0.37	0.76	–	–	–	–	–	–
	60	A	0.71	0.51	0.72	0.68	0.51	0.74	0.61	0.51	0.82	–	–	–
		B	0.58	0.45	0.77	0.59	0.45	0.75	–	–	–	0.33	− 0.10	0.00
		C	0.57	0.48	0.84	–	–	–	0.29	-0.01	0.00	0.64	0.48	0.75
		D	–	–	–	0.57	0.48	0.84	–	–	–	–	–	–
	72	A	0.84	0.59	0.70	0.87	0.59	0.68	0.86	0.59	0.69	–	–	–
		B	0.81	0.60	0.74	0.83	0.60	0.72	–	–	–	0.77	0.25	0.33
		C	0.75	0.66	0.88	–	–	–	0.72	0.30	0.43	0.84	0.66	0.79
		D	–	–	–	0.83	0.58	0.70	–	–	–	–	–	–
	84	A	0.78	0.70	0.90	0.81	0.70	0.87	0.78	0.70	0.90	–	–	–
		B	0.76	0.72	0.95	0.77	0.72	0.94	–	–	–	0.62	0.45	0.72
		C	0.72	0.72	1.00	–	–	–	0.57	0.43	0.75	0.78	0.72	0.93
		D	–	–	–	0.75	0.71	0.94	–	–	–	–	–	–

the values after tightening was completed (the same values as in Tables 2, 3, and 4).

According to Tables 6, 7 and 8, in the case of $T_h = 30$ mm, $S = 72$, 84 mm, it was found that the calculated value tended to capture the experimental value

with approximately ± 10%. However, in other cases, the accuracy of the calculation decreased and was underestimated, but as S increased, the calculated value tended to be slightly closer to the experimental value. This is considered to be, because, when S is 72 mm or greater, the value of $S-\phi$ is sufficiently large, and after the adjacent bolt is tightened, the vertical displacement added to the compressed wood part directly beneath the target bolt is almost 0. On the other hand, when $S=72$ mm or less, the effect received by tightening adjacent bolts is significant, and the vertical displacement added to the compressed wood part directly beneath the target bolt becomes significant. Since Eq. (2) is a function for when the compressed part of the wood has a flat shape, it is considered that it cannot be applied to the geometric change of the compressed part of wood due to the tightening of adjacent bolts. From the above, when S is large, the proposed evaluation formula can ignore the influence of geometric changes. However, the evaluation formula for when S is small will be left as a future subject. In addition, this calculation method does not consider the effects of stress relaxation on wood. It is very difficult to quantitatively evaluate how much stress relaxation affects the fluctuation of axial force due to elastic interactions, but it is speculated that the effect may be greater depending on the material and this could also be investigated in future studies.

Conclusions

Tightening experiments were conducted within the elastic range on multiple bolted joints in a wooden structure with the tightening sequence, bolt spacing, and wood thickness set as parameters and the manner in which each factor affected variations in axial force due to elastic interactions was investigated. The following findings were obtained within the scope of this study:

(1) Variations in axial force tended to be smaller as bolt spacing S increased and it was found that whichever tightening sequence was employed there was a tendency for the axial force of all the bolts to become roughly uniform.
(2) By deriving an evaluation formula that calculates variations in axial force due to elastic interactions and comparing calculated values against experimental values, it was found that for the case of wood thickness $T_h=30$ mm and bolt spacing $S=72$, 84 mm (6d and 7d (where d is the bolt diameter)), the calculated values tended to capture the experimental values well. However, for other cases, the accuracy of the calculated values decreased and was found to be underestimated.

From the above, it was suggested that variations in axial force due to the elastic interaction can be avoided by sufficiently increasing bolt spacing S. On the other hand, the derivation of an evaluation formula considering the case, where the effects of stress relaxation/creep and deformation due to the tightening of adjacent bolts cannot be ignored has become an issue for the future.

Acknowledgements
Not applicable

Author contributions
DM designed and performed the experiments and analyzed the data. MT and YW analyzed the data. All authors read and approved the final manuscript.

Funding
This work was supported in part by the research grant of the Maeda Engineering Foundation.

Availability of data and materials
Not applicable.

Declarations

Ethics approval and consent to participate
Not applicable.

Consent for publication
We agree to allow our manuscript being published.

Competing interests
The authors declare that they have no competing interests.

Author details
[1]Kindai University, 11-6 Kayanomori, Iizuka, Fukuoka 820-8555, Japan. [2]Niigata University, 8050, Ikarashi 2-no-cho, Nishi-ku, Niigata 950-2181, Japan. [3]Toyama Prefectural Agricultural, Forestry & Fisheries Research Center, Imizu, Toyama 4940939-0311, Japan.

Received: 16 June 2022 Accepted: 19 August 2022
Published online: 02 September 2022

References

1. Sawata K (2015) Strength of bolted timber joints subjected to lateral force. J Wood Sci 61:221–229
2. Hirai T (2007) Current issues of timber construction (in Japanese). Mokuzai Gakkaishi 53:117–126
3. Hirai T, Meng Q, Sawata K, Koizumi A, Sasaki Y, Uematsu T (2008) Some aspects of frictional resistance in timber constructions. In: Proceedings of the world conference on timber engineering 2008, Miyazaki, 2–5 June 2008
4. Wakashima Y, Shimizu H, Kitamori A, Matsubara D, Ishikawa K, Fujisawa Y (2019) Stress relaxation behavior of wood in the plastic region under indoor conditions. J Wood Sci 65:1–9. https://doi.org/10.1186/s10086-019-1802-8
5. Wakashima Y, Fujisawa Y, Shimizu H, Kitamori A, Matsubara D, Ishikawa K (2019) Relaxation behavior of wood combined with accelerated treatment and retightening. In: Abstracts of the 69th annual meeting of the Japan wood research society in Hakodate, Hakodate Arena, Hakodate, March 2019
6. Wakashima Y, Shimizu H, Ishikawa K, Fujisawa Y, Tesfamariam S (2019) Friction-based connectors for timber shear walls: static experimental tests. J Archit Eng 25:04019006-1–04019006-9
7. Ishikawa K, Wakashima Y, Fujioka R, Shimizu H, Matsubara D, Kitamori A (2021) Contributions of plywood shear walls and plasterboards on

seismic response reduction of timber structures using wood friction-based dampers (in Japanese). AIJ J Technol Des 27(65):166–171
8. Wakashima Y, Ishikawa K, Shimizu H, Kitamori A, Matsubara D, Tesfamariam S (2021) Dynamic and long-term performance of wood friction connectors for timber shear walls. Eng Struct. https://doi.org/10.1016/j.engstruct.2021.112351
9. Matsubara D, Wakashima Y, Shimizu H, Kitamori A (2020) The load factor in bolted timber joints under external tensile loads. J Wood Sci 66(9):1–7. https://doi.org/10.1186/s10086-020-01857-4
10. Matsubara D, Nakano T, Shimada M, Funada R, Hattori N (2015) Effect of tightening velocity on the torque coefficient of timber jointing with bolts (in Japanese). Mokuzai Gakkaishi 61(1):33–39
11. Matsubara D, Wakashima Y, Fujisawa Y, Shimizu H, Kitamori A, Ishikawa K (2017) Tightening torque calculation method for plastic clamp force of bolted timber joints (in Japanese). Mokuzai Gakkaishi 63:162–175
12. Matsubara D, Wakashima Y, Fujisawa Y, Shimizu H, Kitamori A, Ishikawa K (2017) Relationship between clamp force and pull-out strength in lag screw timber joints. J Wood Sci 63:625–634
13. Matsubara D, Wakashima Y, Fujisawa Y, Shimizu H, Kitamori A, Ishikawa K (2018) Effects of tightening speed on torque coefficient in lag screw timber joints with steel side plates. J Wood Sci 64:112–118
14. Matsubara D, Wakashima Y, Fujisawa Y, Shimizu H, Kitamori A, Ishikawa K (2019) A novel method for estimating ultimate clamp force in lag screw timber joints with steel side plates. Trans Mater Res Soc Jpn 44:109–113
15. Fukuoka T, Takaki T (2001) Finite element simulation of bolt-up process of pipe flange connections. J Press Vessel Technol 123:282–287
16. Nassar SA, Alkelani AA (2006) Clamp load loss due to elastic interaction and gasket stress relaxation and creep in bolted joints. J Press Vessel Technol 128:394–401
17. Alkelani AA, Nassar SA, Housari BA (2009) Formulation of elastic interaction between bolts during the tightening of flat-face gasketed joints. J Mech Des 131:021004
18. Nassar SA, Yang X (2009) Novel formulation of bolt elastic interaction in gasketed joints. J Press Vessel Technol 131:051204
19. Abasolo M, Aguirrebeitia J, Aviles R, Fernandez de Bustos I (2011) A tetra-parametric metamodel for the analysis and design of bolting sequences for wind generator flanges. J Press Vessel Technol 133:041202
20. Bouzid A, Galai H (2011) A new approach to model bolted flange joints with full face gaskets. J Press Vessel Technol 133:021203
21. Abasolo M, Aguirrebeitia J, Aviles R, Fernandez de Bustos I (2014) Methodology for the optimization of bolting sequences for wind generator flanges. J Press Vessel Technol 136:061202
22. Wang YQ, Wu JK, Liu HB, Xu ST (2015) Modeling and numerical analysis of multi-bolt elastic interaction with bolt stress relaxation. Proc IMechE Part C J Mech Eng Sci. https://doi.org/10.1177/0954406215615155
23. Zhu L, Bouzid A, Hong J, Zhang Z (2018) Elastic interaction in bolted flange joints: an analytical model to predict and optimize bolt load. J Press Vessel Technol 140:041202
24. Zhu L, Bouzid A, Hong J (2018) Analytical evaluation of elastic interaction in bolted flange joints. Int J Press Vessel Pip 165:176–184
25. Zhu L, Bouzid A, Hong J (2021) A method to reduce the number of assembly tightening passes in bolted flange joints. J Manuf Sci Eng 143:121006
26. Awaludin A, Hirai T, Hayashikawa T, Leijten A (2012) A finite element analysis of bearing resistance of timber loaded through a steel plate. Civ Eng Dimens 14(1):1–6
27. Matsubara D, Shimada M, Hirai T, Funada R, Hattori N (2016) Embedment of metal washers into timber members of bolted timber joints I. Application of the theory of a beam on an elastic foundation (in Japanese). Mokuzai Gakkaishi 62(4):119–132
28. Teranishi M, Matsubara D, Wakashima Y, Shimizu H, Kitamori A (2021) Nonlinear finite-element analysis of embedment behavior of metal washer in bolted timber joints. J Wood Sci 67(41):1–9. https://doi.org/10.1186/s10086-021-01973-9
29. Kitamori A, Mori T, Kataoka Y, Komatsu K (2009) Effect of additional length on partial compression perpendicular to the grain of wood: difference among the supporting conditions (in Japanese). J Struct Constr Eng (Trans AIJ) 74:1477–1485
30. Matsubara D, Teranishi M (2022) Evaluation of elastic stiffness in bolted timber joints for applying turn-of-nut method. J Wood Sci 68(32):1–7. https://doi.org/10.1186/s10086-022-02038-1
31. Kuwamura H (2012) Anisotropy and densifying effect in bearing stress relaxation of wood: study on steel-framed timber structures Part 13 (in Japanese). J Struct Constr Eng (Trans AIJ) 77:1429–1436

Publisher's Note